

SENSING CAPABILITIES OF LIQUID METAL MAGNETORHEOLOGICAL COMPOSITES

Qingtian Zhang and Weihua Li*

* School of Mechanical, Materials, Mechatronic and Biomedical Engineering
University of Wollongong
NSW, Australia
e-mail: weihuali@uow.edu.au

Abstract. The utilization of elastic conductive materials has become increasingly popular owing to their excellent conductivity and ability to withstand deformation. In this work, a wearable sensor based on a positive piezoconductive composite composed of liquid metal microdroplets, metal microparticles, and elastic matrix is present. This composite is capable of enduring more than 55% compressive strain and 200% tensile strain while maintaining excellent conductivity under any deformation. The resistance of the composite drops sharply to ten-millionth of its initial value with only 20% strain, indicating a remarkable sensitivity to deformation. Based on excellent strain sensitivity of the composite, applications in finger joint detection and gait analysis are developed.

Key words: strain sensors, liquid metals, magnetorheological elastomers, positive piezoconductive effects, wearable electronics.

1 INTRODUCTION

Elastic conductive composites are increasingly becoming popular due to their potential to monitor various physiological signals and human activities [1]-[3]. Generally, a flexible conductive composite is an elastomer matrix filled with conductive fillers, which endows the electrical conductivity from conductive fillers and the good mechanical properties from the polymer elastomer.

Traditionally, the conductive fillers can be divided into four parts: particle filler, flake filler, wire filler, and liquid filler. Composites dispersed with particle fillers such as carbon black and gold nanoparticles [4]-[5], show high strain sensitivity under deformation because the particles can easily separate with each other. Flake and wire fillers like silver microflakes and silver nanowires [6]-[7] with the high aspect ratio can overlap during the deformation to maintain high conductivity, but they are insensitive to strain. Recently, gallium-based liquid metal alloys have been used widely in fabricating conductive elastomers due to their high conductivity and high flexibility [8]. However, as most of the literature reports, the conductive elastomer uses these fillers, its resistivity increases when subjected to an external force to produce strain [9]-

[11]. Therefore, a conductive elastomer with reduced resistivity under tension or compression is required.

A promising new type of composite material called liquid metal magnetorheological elastomer (LMMRE) has recently emerged. Unlike most conductive elastic materials, LMMRE experiences a drastic drop in resistance after being strained by an external force, making it an ideal candidate for stretchable sensors. Additionally, a novel liquid metal and irregular nickel powder-filled magnetorheological elastomer (E-Ni-LMMRE) is introduced in this work. This composite is capable of enduring more than 55% compressive strain and 200% tensile strain, while maintaining excellent conductivity under any deformation. The resistance of the composite drops sharply to ten-millionth of its initial value with only 20% strain, indicating a remarkable sensitivity to deformation. Finally, two functional wearable haptic devices based on novel compressive and tensile strain sensitivity of this composite are developed and characterized, with a focus on enhancing communication and injury recovery, respectively.

2 MATERIALS AND METHODS

2.1 Materials and Fabrications

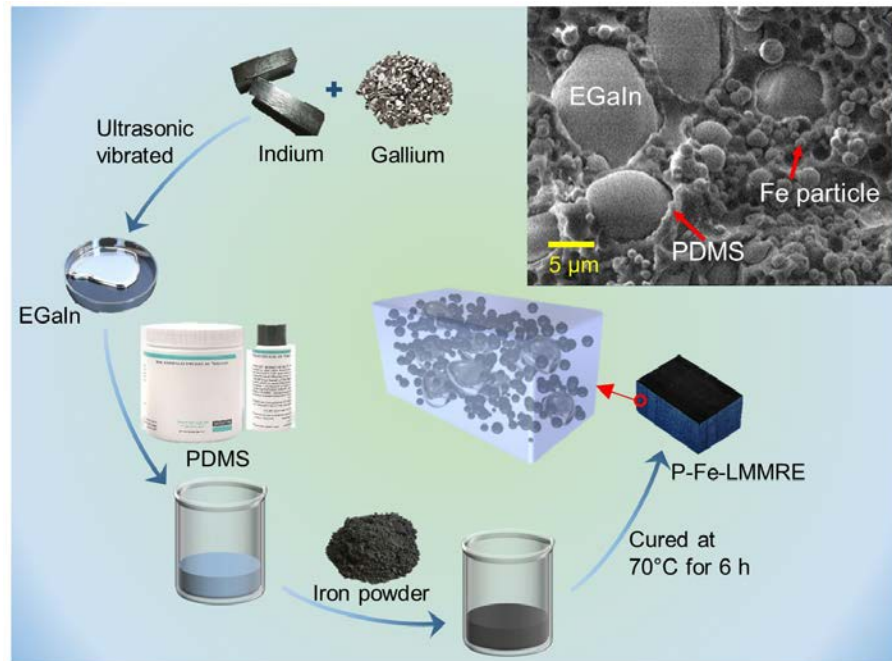


Figure 1. The fabrication method, 3D microstructure, and scanning electron microscopy (SEM) of P-Fe-LMMRE.

Figure 1 illustrates the fabrication method, 3D microstructure, and scanning electron microscopy (SEM) of P-Fe-LMMRE. EGaln are composed of gallium (75%wt) and indium (25%wt) mixed and vibrated. The raw materials of the P-Fe-LMMRE samples are PDMS (curing agent/PDMS base mass ratio of 1:9), iron powder, and EGaln. We put the raw materials

(the mass ratio is 1:4:1) into a transparent plastic cup in order and use an electric stirrer equipped with a plastic rod (diameter of 4 mm) to stir at a speed of 400 rpm for 2 minutes. Due to many sets of experiments, the specific weight of raw material is determined according to actual needs. Then, we use a vacuum pump to remove air bubbles in the mixture for 10 minutes and poured the mixture into Acrylic molds ($8 \times 8 \times 8$ mm for bulk and $3 \times 5 \times 30$ mm for strip). The mixture is cured in an oven (70°C) for 6 h to obtain the P-Fe-LMMRE. The E-Ni-LMMRE sample consists of Ecoflex, nickel powder, and EGaIn. Following the order of A liquid-EGaIn-nickel powder-B liquid, we mix the raw materials to prevent the beforehand cure of Ecoflex. After that, we stir the mixture manually by plastic rod until it mixed uniformly and pour it into Acrylic molds ($8 \times 8 \times 8$ mm for bulk and $3 \times 5 \times 30$ mm for strip). The E-Ni-LMMRE is cured after 6 h at room temperature.

2.2 Experimental Equipment and Instruments

A VLS2.30 Laser Cutter (Universal Laser Systems) and a formlabs form 3 3D printer are used to prepare molds. A JEOL JSM-6490LA scanning electron microscope is employed to get the SEM images. An MTS Landmark 370.02 hydraulic load frame is used to measure the stress-strain curves of composites. The Instron ElectroPulsTM E3000 Linear-torsion electric dynamic test instrument equipped with pneumatic clamps is used to perform the tensile limitation tests on the standard tensile samples ($2 \times 6 \times 30$ mm for the stretched part). A SyringePump Screw Driven Linear Guide is used to compress and stretch the P-Fe-LMMRE and E-Ni-(LM)MRE samples. A VICI Digital Multimeter (VC8145) with a resistance range of $80\text{ M}\Omega$ was used to measure the resistance of the samples. The compressive tests use bulk composites ($8 \times 8 \times 8$ mm) and the tensile tests (included tensile limit tests) use strip composites ($3 \times 5 \times 30$ mm), which are compressed and stretched at the speed of $0.021\text{ mm}\cdot\text{s}^{-1}$ and $0.052\text{ mm}\cdot\text{s}^{-1}$, respectively. The finger joint detect device is composed of a rubber glove, wires, and film E-Ni-LMMRE samples ($1.8 \times 3.5 \times 45$ mm). The gait analysis equipment is made by a block E-Ni-LMMRE ($10 \times 10 \times 6$ mm) with two silver tapes embedded in a circle Ecoflex substrate (with a diameter of 50 mm and thickness of 6 mm).

3 RESULTS AND DISCUSSION

3.1 Mechanical properties of LMMRE

The first experiment carried out is to investigate the mechanical characteristics of P-Fe-LMMRE and E-Ni-LMMRE. Figure 2 displays the stress-strain patterns during cyclic compression and tension for both P-Fe-LMMRE and E-Ni-LMMRE. The loading and unloading curves do not coincide, demonstrating elastic-plastic behavior similar to that of rubber. The gradient of the curves increases with an increase in strain, indicating a conspicuous stress amplification phenomenon. The unloading curve reveals that the specimen can almost revert to its original state. Additionally, the size of the elastic hysteresis loop created by the loading/unloading curve is small, indicating that the composite experiences less energy dissipation throughout the cycle. The 1st cycle and 2nd cycle are highly overlapping indicating the good durability of the composites. E-Ni-LMMRE has a significantly lower elastic modulus

compared to P-Fe-LMMRE. Its maximum stress is only 0.149 MPa at a compressive strain of 20%. Under the same strain, the stress of E-Ni-LMMRE is only about one-fortieth of that of P-Fe-LMMRE. Moreover, the elastic hysteresis loop area of E-Ni-LMMRE is smaller, demonstrating lower energy loss. The E-Ni-LMMRE displays more stretchable and flexible than P-Fe-LMMRE when tension, embodied in 202% of the tensile limit and 0.68 MPa tensile strength and 38.4% of the tensile limit and 3.5 MPa tensile strength, respectively. The cross-linking of the matrix largely caused the difference in the mechanical properties of these two elastic composites. The cross-link density of Ecoflex is lower than that of PDMS, leading to a lower mechanical modulus softer mechanic structure of E-Ni-LMMRE. Therefore, the soft E-Ni-LMMRE with lower metal content and lower cross-link density than P-Fe-LMMRE is more suitable for the wearable sensors.

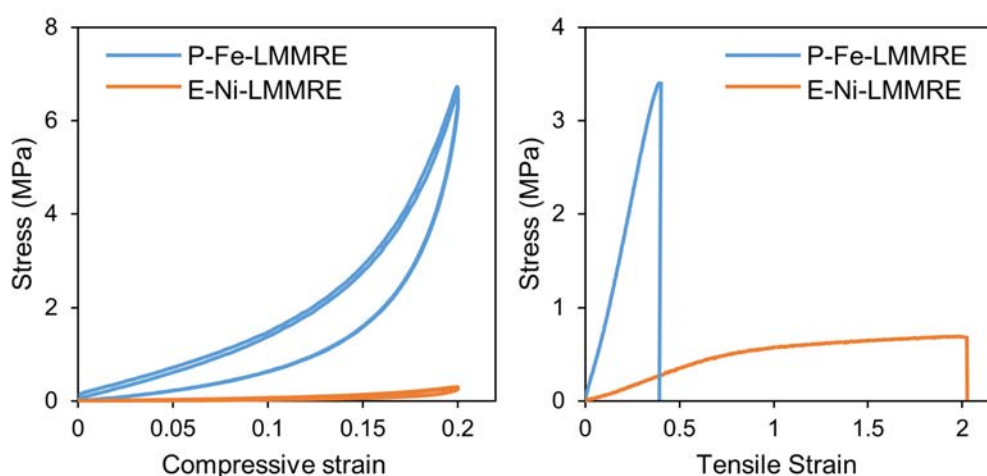


Figure 2. Strain-stress curves of P-Fe-LMMRE & E-Ni-LMMRE under cyclic compression and tension.

3.2 Electrical properties of LMMRE

Figure 3 displays the resistivity-strain curves of P-Fe-LMMRE and E-Ni-LMMRE samples during compression and tension, respectively, with a logarithmic strain axis. The P-Fe-LMMRE composite exhibits good conductivity at small strains (< 0.1) thanks to its relatively high metal powder content, and its resistivity drops exponentially. However, as the compression increases, the curve's trend gradually decreases, indicating slow resistance reduction. At a strain of 0.2, the resistivity of E-Ni-LMMRE decreases sharply from $10 \text{ M}\Omega\cdot\text{m}$ to nearly $10 \text{ }\Omega\cdot\text{m}$, with a significantly greater decline than that of P-Fe-LMMRE. Similarly, in the tensile test, the resistivity of P-Fe-LMMRE and E-Ni-LMMRE decrease by 2 and 6 orders of magnitude, respectively, within 10% tensile strain. Additionally, these resistivity curves fit well with the power trend lines (coefficients of determination $R^2 > 0.99$). The lack of symmetry between the compression and tension curves of the same sample is due to differences in clamping during the two experiments. In the tensile test, the pre-pressure applied at both ends of the strip sample

causes the initial resistivity of the sample to decrease by nearly an order of magnitude compared to the compression test. Furthermore, the effect of the pre-pressure is reflected in maintaining the rate of resistivity decline. In conclusion, E-Ni-LMMRE has a higher initial resistance than P-Fe-LMMRE but exhibits better strain sensitivity.

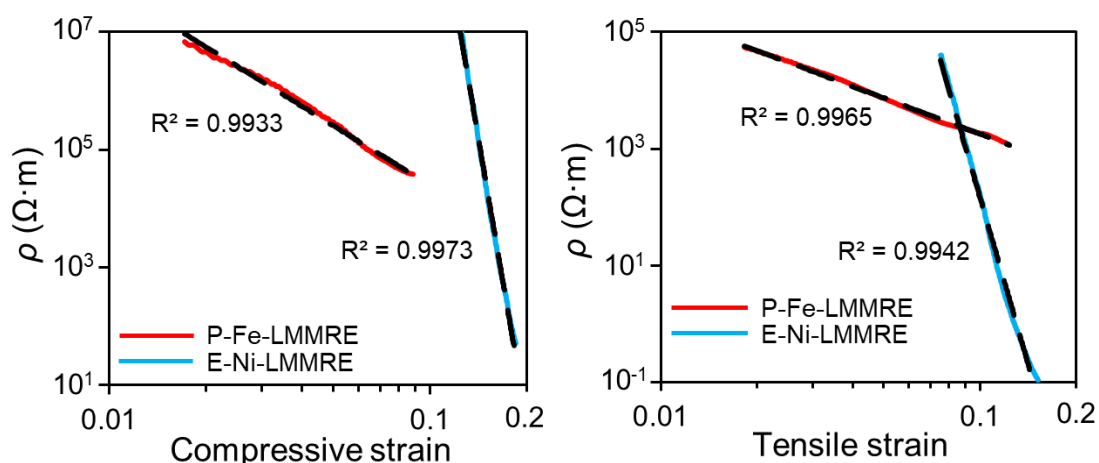


Figure 3. Resistivity-strain curves of P-Fe-LMMRE sample and E-Ni-LMMRE sample under compression and tension.

We present SEM of E-Ni-LMMRE and draw a schematic diagram to explain why it has higher strain sensitivity than P-Fe-LMMRE. As shown in Figure 4, the shape of Ni particles is not as smooth as spherical Fe particles shown in Figure 1, but has a large number of spike-shaped structures on the surface like a sea urchin. These spike structures can provide more electrical contact opportunities for adjacent nickel particles to significantly improve the overall electrical conductivity of the composite. Therefore, composites filled with spike-shaped nickel particles exhibit higher sensibility in comparison to that filled with smooth iron particles.

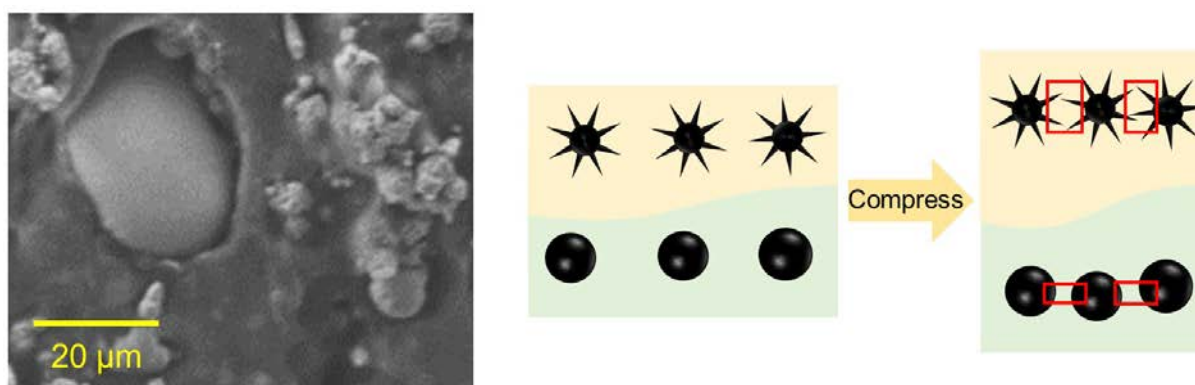


Figure 4. The SEM of E-Ni-LMMRE and change in the microstructure of the E-Ni-LMMRE and P-Fe-LMMRE under compression.

4 APPLICATIONS OF LMMRE

4.1 Finger joint detect device

The LMMRE strip sensors are developed to detect human finger joint bending angles. To achieve this, the sensors are fixed on the tester's finger with tape and bent over a fixed angle range. However, due to the low conductivity at small strains (< 0.02 for P-Fe-LMMRE and < 0.07 for E-Ni-LMMRE), the tester needs to pre-bend the sensors to a certain degree to decrease resistance (15° for P-Fe-LMMRE and 30° for E-Ni-LMMRE). As depicted in Figure 5(a), when the index finger bends, the sensors deform and their resistance drops rapidly. The P-Fe-LMMRE sensor has a larger degree range (15°) compared to the E-Ni-LMMRE sensor. However, the E-Ni-LMMRE sensor shows a more distinct difference between adjacent scales, indicating its more accurate bending angle recognition ability.

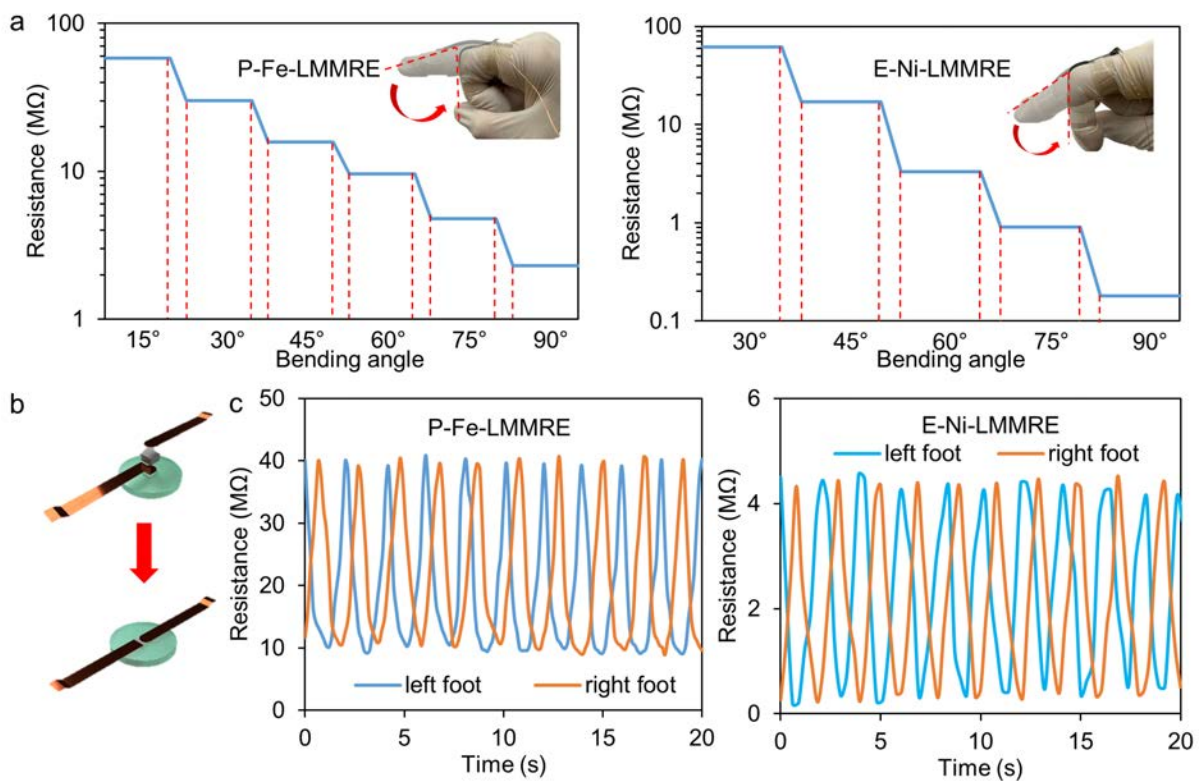


Figure 5. (a) The resistance-bending angle curves by using the P-Fe-LMMRE and E-Ni-LMMRE sensors. (b) Sketch of the gait analysis device. (c) The curve of resistance versus time of P-Fe-LMMRE and E-Ni-LMMRE sensors under walking test.

4.2 Gait analysis equipment

To harness the good compressive strain sensitivity of LMMRE, we have developed a gait analysis equipment to monitor human gait. The schematic of the gait analysis equipment is presented in Figure 5(b), and the device is placed as an insole at the human's heel. Ecoflex was

chosen as the base layer due to its excellent softness and flexibility, which increases the comfort of the wearer. Figure 5(c) shows the walking electrical response for healthy individuals. However, the P-Fe-LMMRE sensor had a high Young's modulus, which caused it to only experience a small strain ($< 4\%$) during walking, leading to a resistance of more than $10\text{M}\Omega$. According to Ohm's Law, the resistance of the sensor would result in smaller current under the same voltage. As a result, the microcontroller's current accuracy could become a limiting factor, resulting in inaccurate results. Therefore, the relatively high resistance of the P-Fe-LMMRE sensor might restrict its potential in microcontroller-based applications.

On the other hand, the E-Ni-LMMRE sensor exhibited excellent performance due to its low resistance range (from 0.1 to $4.5\text{M}\Omega$). Its low Young's modulus allowed it to experience larger compressive strains during the walking test, which resulted in a greater reduction of resistance. Additionally, the numerous electrical contact points between the irregular nickel particles further enhanced the positive piezoelectric effect in the E-Ni-LMMRE sensor. Consequently, the E-Ni-LMMRE sensor showed low resistance and was suitable for microcontroller-controlled applications.

5 CONCLUSIONS

Two types of MRE composites filled with hybrid conductive fillers are presented in this work. When stretching/compressing the composites, the conductive fillers in the composites squeeze the elastic matrix layers to form more conductive paths, reducing the resistance rapidly. The E-Ni-LMMRE was extremely stretchable and sensitive to mechanical deformation owing to the excellent mechanical properties of Ecoflex and the electrical connection among irregular Ni particles, respectively. Taking advantage of the unique properties of the LMMRE, two devices for monitoring human motion are reported based on the sensitivity of tension and compression respectively.

REFERENCES

- [1]. Y. Zheng, Y. Li, K. Dai, Y. Wang, G. Zheng, C. Liu, and C. Shen, "A highly stretchable and stable strain sensor based on hybrid carbon nanofillers/polydimethylsiloxane conductive composites for large human motions monitoring," *Composites Science and Technology*, vol. 156, Mar., pp. 276-286, 2018.
- [2]. X. Liao, Z. Zhang, Z. Kang, F. Gao, Q. Liao, and Y. Zhang, "Ultrasensitive and stretchable resistive strain sensors designed for wearable electronics," *Materials Horizons*, vol. 4, no. 3, pp. 502-510, 2017.
- [3]. S. Lee, S. Shin, S. Lee, J. Seo, J. Lee, S. Son, H. J. Cho, H. Algadi, S. Al-Sayari, D. E. Kim, and T. Lee, "Ag Nanowire Reinforced Highly Stretchable Conductive Fibers for Wearable Electronics," *Advanced Functional Materials*, vol. 25, no. 21, Jun., pp. 3114-3121, 2015.
- [4]. Y. Fu, F. Yi, J. Liu, Y. Li, Z. Wang, G. Yang, P. Huang, N. Hu, and S. Fu, "Super soft but strong E-Skin based on carbon fiber/carbon black/silicone composite: Truly

- mimicking tactile sensing and mechanical behavior of human skin,” *Composites Science and Technology*, vol. 186, Jan., pp. 107910, 2020.
- [5]. Y. Kim, J. Zhu, M. D. Prima, X. Su, J. Kim, S. J. Yoo, C. Uher, and N. A. Kotov, “Stretchable nanoparticle conductors with self-organized conductive pathways,” *Nature*, vol. 500, no. 1, pp. 59-63, 2013.
 - [6]. S. Ding, J. Ying, F. Chen, L. Fu, Y. Lv, S. Zhao, and G. Ji, “Highly stretchable conductors comprising composites of silver nanowires and silver flakes,” *Journal of Nanoparticle Research*, vol. 23, pp. 111, 2021.
 - [7]. C.-Y. Huang, Y.-C. Lai, and Y.-C. Liao, “Photocurable Stretchable Conductors with Low Dynamic Resistance Variation,” *ACS Applied Electronic Materials*, vol. 1, no. 5, pp. 718-726, 2019.
 - [8]. N. Kazem, M.D. Bartlett, and C. Majidi, “Extreme Toughening of Soft Materials with Liquid Metal,” *Advance Materials*, vol. 30, no. 22, pp. e1706594, 2018.
 - [9]. L. Chen, G.H. Chen, and L. Lu, “Piezoresistive Behavior Study on Finger-Sensing Silicone Rubber/Graphite Nanosheet Nanocomposites,” *Advanced Functional Materials*. Vol. 17, no. 6, pp. 898-904, 2007.
 - [10]. H. Chen, Z. Su, Y. Song, X. Cheng, S. Chen, B. Meng, Z. Song, D. Chen, and H. Zhang, “Omnidirectional Bending and Pressure Sensor Based on Stretchable CNT-PU Sponge,” *Advanced Functional Materials*, vol. 27, no. 3, 1604434, 2017.
 - [11]. Y. Yoon, K. Samanta, H. Lee, K. Lee, A. P. Tiwari, J. Lee, J. Yang, and H. Lee, “Highly Stretchable and Conductive Silver Nanoparticle Embedded Graphene Flake Electrode Prepared by In situ Dual Reduction Reaction,” *Scientific Reports*, vol. 5, 14177, 2015.